Journal of Energy Storage 88 (2024) 111649

Contents lists available at ScienceDirect

Journal of Energy Storage

journal homepage: www.elsevier.com/locate/est

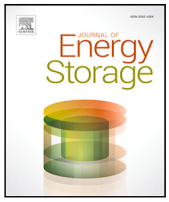

Research papers

State-of-Health prediction of lithium-ion batteries based on a low dimensional Gaussian Process Regression

Sebastian Pohlmann [a,*], Ali Mashayekh [b], Florian Stroebl [c], Dominic Karnehm [a], Manuel Kuder [d], Antje Neve [a], Thomas Weyh [b]

[a] University of the Bundeswehr Munich, Institute of Distributed Intelligent Systems, Werner-Heisenberg-Weg 39, Neubiberg, 85577, Bavaria, Germany
[b] University of the Bundeswehr Munich, Institute of Electrical Energy Systems, Werner-Heisenberg-Weg 39, Neubiberg, 85577, Bavaria, Germany
[c] University of Applied Sciences Munich, Institute for Sustainable Energy Systems, Lothstraße 64, Munich, 80335, Bavaria, Germany
[d] BAVERTIS GmbH, Marienwerderstraße 6, Munich, 81929, Bavaria, Germany

ARTICLE INFO

Keywords:
Lithium-ion battery
State of health
Machine learning
Gaussian Process Regression

ABSTRACT

An accurate determination of the condition of a battery is a key challenge in operation. As the performance of lithium-ion batteries is degrading over time, an accurate prediction of the State-of-Health would improve the overall efficiency and safety. This paper presents a prediction method for the State-of-Health based on a Gaussian Process Regression with an automatic relevance determination kernel in a single model for three different types of battery cells. After reducing the dimension of the problem and a sensitivity analysis of the features, the model is trained, validated, and further tested on unseen data. A minimum test error is obtained with a mean absolute error of 1.33%. Combined with the low uncertainty of the prediction results, this shows the applicability and the great potential of forecasting the condition of a battery using data-driven methods.

1. Introduction

One of the biggest challenges society is currently facing is the reduction of greenhouse gas emissions. In combination with the government policy requirements, the general move to renewable energy and the electrification of the transport sector is inevitable [1]. Due to their long lifetime and their high energy density, lithium-ion batteries (LIBs) have taken on a predominant role in the automotive industry [2]. To maximize the efficiency, achieve a high driving range, and ensure a safe and reliable operation, it is crucial to determine the condition of a battery [3,4]. As LIBs are complex electrochemical systems and are facing a high variety of operating and loading conditions, it is a key problem to accurately predict the State-of-Health (SOH) [5]. During battery ageing, the battery performance degradation is caused by various intertwined factors. The variety of cell manufactures and submaterials, as well as the complexity of the manufacturing process result in structurally and physically different cells, even for battery cells of the same kind [6,7]. To determine the SOH of a battery cell, two main methods can be distinguished: model-based and data driven [6,8]. Equivalent circuit model (ECM) based methods are widely applied. They do not consider the chemical composition of the cell, but they approximate the behavior of the cell as a combination of basic electronic components [9]. High efforts are necessary to determine the parameters of the model, and based on the desired accuracy, the complexity of the models vary widely [10]. The ECM based methods are often combined with filtering algorithms, for example Kalman filter to estimate the SOH [11]. Data driven methods do not require to approximate the complex internal electrochemical processes under uncertain working conditions. They are only dependent on the data basis, which should reflect the battery behavior. Disadvantages are the time and cost intensive aging tests to obtain the data [12]. A huge and reliable dataset is necessary to train the machine learning (ML) methods and to select the optimal hyperparameters for predicting the target values. Advances in computational power and data generation are driving factors for the success of statistical and ML algorithms [13]. Especially in the context of a big data platform in the vehicle field, health monitoring of LIBs based on ML can profit from the huge amount of data and can result in highly accurate models [12].

There are several approaches to estimate the SOH of LIBs based on data-driven methods because of their ease of use and the potential to optimize the resulting models, as more data becomes available [14,15]. In comparison to physical models, the complex electrochemical processes do not have to be modeled. On the one hand, data-driven approaches are concentrating on artificial neural networks [16–19], and in that field mainly on long short-term memory (LSTM) networks [20,21]. On the other hand, probability models gain high interest for predicting the condition of a battery resulting in robust models with

* Corresponding author.
E-mail address: sebastian.pohlmann@unibw.de (S. Pohlmann).

https://doi.org/10.1016/j.est.2024.111649
Received 5 October 2023; Received in revised form 14 March 2024; Accepted 6 April 2024
Available online 11 April 2024
2352-152X/© 2024 The Author(s). Published by Elsevier Ltd. This is an open access article under the CC BY license (http://creativecommons.org/licenses/by/4.0/).

high accuracies [22,23]. Main representative of these model types are a Gaussian Process Regression (GPR) [24–26]. Another advantage of those models is that it is not only possible to predict the condition of a battery, but also to express the uncertainty of the estimated results. The results are not only a function for target values $y = f(x)$, but they also show the distribution $(y|x)$ of the prediction [27].

Richardson et al. [28] extracted features manually to predict the SOH using a GPR. They consider the integrated current through the cell as well as time elapsed during the loading pattern. With the matern kernel for handling varying degrees of smoothness, they reach a root mean square error (RMSE) of the model of 4.3%. Similar to that, Feng and Shi [29] manually extracted features from the charging patterns of the battery and trained their model based on five features. The features consist of the times of the loading pattern and the change in current and capacity with the highest correlations between the current change and the SOH. They also use a combined kernel function for long term decrease, fluctuations, and noise and obtain error values below 3%. Yang et al. [30] extract four features with the times of constant current and constant voltage phase and the two slopes of the charging curves to train a GPR with two squared exponential functions as the kernel. The model results in errors below 6%. In contrast to the approaches with manual feature extraction, Tagade et al. [31] developed a deep GPR with an automatic feature extraction method for capacity and end of life prediction. They used a random sequence of time, voltage, and temperature and extracted the features with the hidden layers of a deep learning network. The results show mean absolute errors (MAE) below 10%. Further, they observe high correlations between the outputs of the hidden layers and the internal battery parameters, indicating the applicability of automatic feature extraction methods. Greenbank et al. [32] used the data distribution of the time series of voltage, current, and temperature and calculated the four different percentiles as input features. When estimating the capacity, they reach errors below 2%. For many approaches in the literature, the open source datasets available from the NASA Ames Prognostics Center of Excellence repository are utilized. On the one hand, this emphasizes the need for reliable battery ageing data or data improvement and augmentation methods, yet on the other hand, it improves the comparability of different models. Next to the data and the feature extraction, a key point is the selection of a suitable kernel. The accuracy of a prediction model based on different kernel functions is analyzed by Liu et al. [33]. They perform the prediction on calendar aging data under different conditions and conclude that the automatic relevance determination (ARD) kernel, specifically a matern kernel, is most suitable for a forecasting model based on calendar aging data. Overall, despite its high sensitivity against hyperparameter, the matern kernel is commonly used for the SOH estimation, as it is easy to control the smoothness of the functions and the ability to approximate local and globally varying functions [28,32,34,35].

The contribution of this paper is the novel approach to develop a prediction model for the SOH for different battery types, the comparison of feature pre-processing methods, and the development of the kernel function. Our own dataset of ten battery cells is used and enlarged by a public dataset of four more cells. As the cells are operated under different conditions, the dataset offers a wide variety of battery degradation. The field of electrical energy storage is highly relevant in current research, but most prediction models are only trained and validated for one battery type. The adaptability to technological leaps and the flexibility between different types are key advantages of the proposed model. This approach can be explained as transfer learning in the field of battery analysis, where, in this case, the results of one battery type can be exploited to improve the prediction for other battery types. Therefore, all data sets are upfront splitted in training, validation, and test data sets. The prediction model is then trained with one battery type and two times retrained for the other battery types. The used values are direct measurements with current, voltage, and temperature. To reduce the risk of overfitting, the dimension of the problem is reduced. Instead of manually extracting the features, two different approaches to create features are compared. Next to a principal component analysis (PCA) to reduce the dimension by analyzing the variance, the number of included timesteps for the prediction and the impact on over- and underfitting is examined. This is done by analyzing the correlation between time steps and target values and then evaluating the impact on the model results. The detailed and accurate extraction of features is crucial for a reliable model with low forecasting errors. Moreover, an oversampling strategy is performed to investigate the effect of artificially created data on the prediction model. The results of the model based on standard metrics are presented in Section 3 and discussed in aspects of an application and data-driven optimization of the model.

2. Materials and methods

Data pre-processing is the key to a successful prediction model, as it is the process from the data selection to the creation of features for training a ML model. The proposed model is a GPR with the pre-processed values of voltage, current, and temperature as features and the SOH as the target value.

2.1. Data origin

LIBs are subject to inevitable aging during operation. The aging behavior is influenced by several operating and environmental conditions [36,37]. To develop a ML model for predicting the SOH, it is important to use reliable data over the whole cycle life of a battery cell. In this case, different data sources are used to train and test the SOH prediction model. All in all, the aging data of 14 different battery cells are used. The aging experiments are conducted using five cells of battery type A (Sony US18650VTC5) and five cells of battery type B (Samsung INR18650 25R). Both cells are 18 650 lithium-ion battery cells with the same cell chemistry (LiNiMnCoO2), but have slight differences in capacity and maximum discharge current. As battery cells are complex electrochemical systems, there is an additional variation in the aging behavior within one cell type. All ten cells are charged in CC-CV mode with 4 A and 0.1 A cut-off for the CV phase. They were discharged with a constant current of 10 A within a voltage range between 2.5 V and 4.2 V to represent high load scenarios [38]. The cells are cycled in a temperature chamber at 25 °C. Next to current and voltage, the temperature of the cells is measured. The temperature curve during the discharge cycle over the aging process for an exemplary cell is shown in Fig. 1. The temperature is plotted against the state of charge (SOC) and the SOH is indicated by the color.

The capacity decrease of the battery cells can be characterized by the SOH, see (1), which is the ratio between the remaining capacity Q_{now} and the capacity at the begin of life Q_{BOL}.

$$SOH = \frac{Q_{now}}{Q_{BOL}} \tag{1}$$

The decrease of the SOH over charging and discharging cycles of the ten cells is shown in Fig. 2. The type A cells in this case have a higher variety in the aging behavior. On the contrary, the degradation curves of the type B cells are overlapping.

Additionally to this data, a public dataset from the NASA prognostics data repository is used [39]. Four commercial 18 650 Lithium-Ion batteries were cycled using a sequence of charging and discharging currents between ±4.5 A. To determine a value for the SOH, reference charge and discharge cycles are performed after 1500 periods of random walk loading operations [40]. As the cells are not charged and discharged with a constant current, the data is closer to a real world application. Only the data of the last reference discharge cycle is used to predict the SOH. Overall, the battery cells data show a wide variety to cover a broad range of operating conditions and even different cell types.

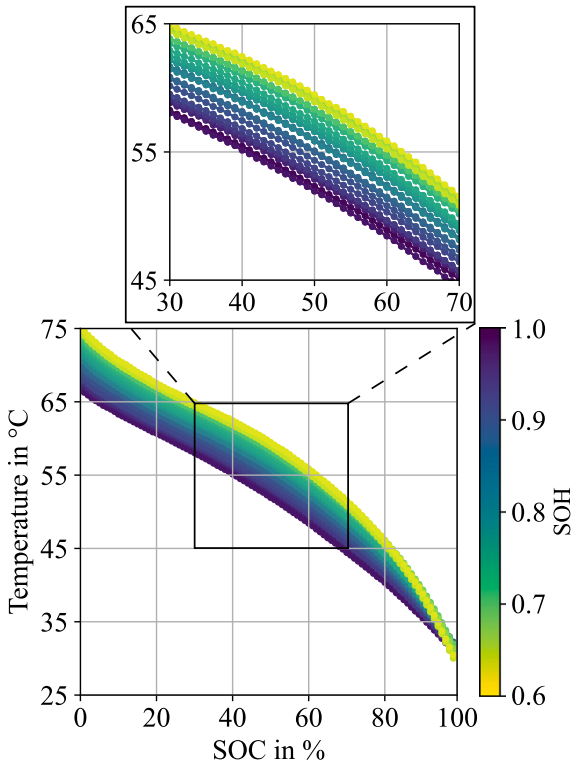

Fig. 1. Temperature profile of a battery cell during discharging with constant current over the cycle life. Every 30th discharge cycle is plotted till the end of life of the cell.

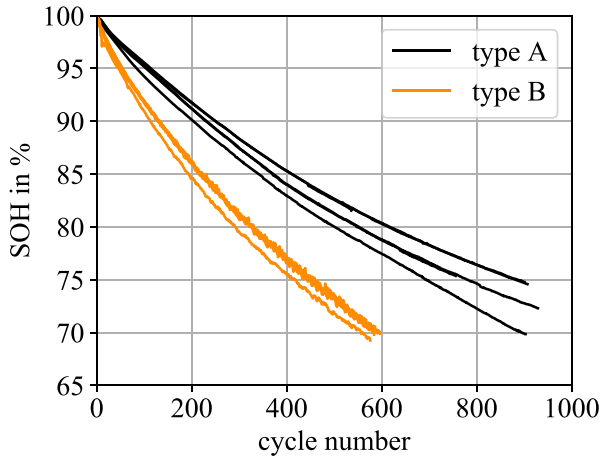

Fig. 2. Aging behavior of the battery cells from the own dataset. The decrease of the SOH is plotted over the cycles during aging experiments for five battery cells each. All ten cells are loaded in CC-CV mode.

2.2. Feature extraction

The input data points for a ML model are called features. The process of selecting these features from the raw data is highly important for a prediction model with low error rates. First, the data of each battery type is separately split into a training and a test dataset with the ratio 80:20. The training data is further subdivided into the final training and validation data with a ratio of 90:10. The validation data is not used for the training, but it is utilized to tune the parameters of the model. Next step in the data preparation process is the scaling of the data. The data points x_i are normalized using the standard deviation s and the mean values $\overline{x}$ of the data distribution resulting in the scaled input features x_i^n, see (2) [41].

$$x_i^n = \frac{x_i - \overline{x}}{s} \tag{2}$$

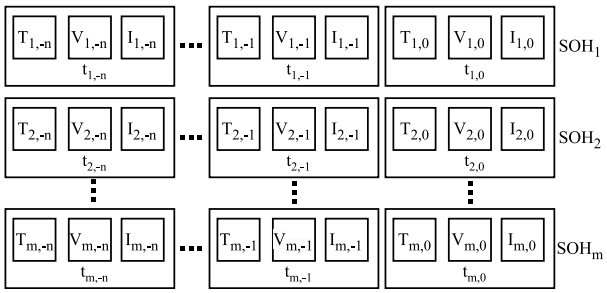

Fig. 3. Initial feature matrix with the data of n timesteps for m SOH values. One timestep t consists of a value for temperature T, voltage V, and current I.

The feature matrix rows contain values for voltage, current, and temperature for up to over 90 time-steps for a single discharge cycle. In sum, the initial feature data consists of voltage, current, and temperature for a whole discharge cycle with a sample rate of 10 s. The initial feature matrix is shown in Fig. 3. One timestep t contains values for temperature T, voltage V, and current I. Starting with the actual timestep at the end of a discharge cycle, the timesteps go back in the past, which is indicated by the negative sign. Each row defines the input values estimating one SOH value.

The data is used to predict the target values for the SOH of the battery. The target vector has the length of 7581 for all reference SOH values. This implicates that the number of features for one target value is smaller than the number of target values, but it is roughly in the same order of magnitude. Similarly, in the context of the "curse of dimensionality" and to reduce the risk of overfitting, it is favorable to reduce the dimension of the problem. In comparison to other ML models, GPRs are typically not so prone to overfitting, but not immune to it. Therefore, the trade-off between improving the model and the risk to drop valuable information has to be assessed in detail. Two methods are pursued. Firstly, the dimension of a whole data batch is reduced by a PCA and, secondly, the number of timesteps included in the feature matrix is decreased. A PCA is a common method to reduce the dimension by analyzing the variance of the different components and including only the relevant components of the feature matrix. It is a technique to reduce the dimension of a feature matrix while removing highly inter-correlated data. The information content is measured using the variance. The data is linearly transformed into a new coordinate space with a lower dimension, but a remaining variance in the dataset. The PCA is closely related to the singular value decomposition (SVD), which is a factorization of the feature matrix M in two orthogonal matrices U and V, and a diagonal matrix $\sum$ with the singular values σ, which are the square roots of the eigenvalues λ [42]. This is shown in (3).

$$M = U \sum V^{\top} \tag{3}$$

The orthogonal matrix V is the orthonormal basis of the eigenvectors of $M^{\top}M$. The matrix U can be calculated with (4).

$$u_i = \frac{1}{\sigma_i} M v_i \tag{4}$$

A SVD is usually computationally more efficient than an eigen decomposition of the covariance matrix, and it can be used to perform a PCA because of the relation between singular and eigenvalues.

Next to the PCA, the included timesteps for the prediction are reduced. Starting with a timeseries of 90 timesteps, the number is decreased while analyzing the correlation between the measured values of different timesteps with the target value. This dimension reduction

approach results in a feature matrix that only contains data in a low state of charge (SOC) range. General aim is to use only a short period of time to keep the prediction model simple and to reduce the risk of overfitting.

Further, an oversampling algorithm is used to enrich the data basis and to optimize the prediction model. The algorithm "Synthetic Minority Over-Sampling Technique for Regression with Gaussian Noise" (SMOGN) is used [43]. A relevance function correlates the target values with a relevance scale in the range between 0 and 1 to enrich the data basis in certain areas [44]. The data above a pre-defined threshold are used for an oversampling process. Depending on the distance between the seed sample and the k-nearest neighbors, the technique "Synthetic Minority Over-Sampling for Regression" (SMOTER) [45] is applied or a new example with Gaussian noise on the seed example is generated [46]. The impact of the method on the prediction model is analyzed and discussed in Section 3.

2.3. Gaussian process regression

A GPR is a Bayesian approach to estimate a distribution over possible functions with the aid of prior knowledge [47]. Key advantage is the robust learning from small training sets, where the dimension of the model is similar or greater than the amount of data points to train the model. GPRs result in a predictive distribution and not a single value, and they are based on kernel functions between the input examples. The hyperparameter of the kernels can be learned by maximizing the likelihood of the training data and, therefore, it is typically more efficient than other hyperparameter optimization techniques, like a grid search [48]. The general goal of a GPR is to recover a function between variables with an error ϵ for N data points $\{(x_i, y_i)\}_{i=1}^{N}$, see (5) [49].

$$y_i = f(x_i) + \epsilon_i \tag{5}$$

The problem is solved by parameterizing the function f with weight parameters w for H basis functions $\{\phi_h(x)\}_{h=1}^{H}$.

$$f(x) := \langle \phi(x), w \rangle \tag{6}$$

A likelihood function for an output vector Y is created, and the associated noise terms s_{noise} are assumed to be independent and normally distributed.

$$p(Y|f_x) = \prod_{i=1}^{N} p(y_i|x_i, f) = \mathcal{N}(Y|f_x, c^2 I) \tag{7}$$

With an Gaussian process prior over the functions in (8), the results are shown in (9) with the terms in (10) and (11), where f can be sampled for the joint posterior distribution by determination of the mean and the covariance matrix K.

$$f \sim GP(m(x) \equiv 0, k(x, x')) \tag{8}$$

$$f|X, Y, x' \sim GP\left(\overline{f}, cov(f)\right) \tag{9}$$

$$\overline{f} = k(x', X)[K + s_{noise}^2 I]^{-1} Y \tag{10}$$

$$cov(f) = k(x', x') - k(x', X)[K + s_{noise}^2 I]^{-1} k(X, x') \tag{11}$$

In (10) and (11), $k(X, x')$ and $k(x', X)$ are kernel functions with the training points as input. K denotes the Gram matrix with the elements $K_{ij} = k(x_i, x_j)$.

To convert the distribution prediction to a point prediction, a loss function L is used. By minimizing the loss, the optimal solution predicting target values y^* based on new input data x^* is calculated, which, for the symmetric loss function, is the mean of the predictive distribution μ^*. To calculate this, the transposed kernel vector $k_{X,x^*}^{\top}$, the covariance matrix K, a noise term s_{noise}^2, and the identity matrix Y are used.

$$y_{optimal}|x^* = argmin \int L(y^*, y_{prediction}) \times p(y^*|x^*, X, Y) dy^* \tag{12}$$

$$\mu^* = k_{X,x^*}^{\top}(K + s_{noise}^2 I)^{-1} Y \tag{13}$$

The kernel functions are chosen to best approximate the data distribution. There are several factors, which have to be taken into account while choosing the appropriate kernel function. Instead of an isotropic kernel, an automatic relevance determination (ARD) kernel is used. An isotropic function is commonly used as kernel as they work well for interpolating smooth functions, but it has limitations as it only depends on the distance between kernel arguments and not on the direction, as shown in (14) [50].

$$k(x, x') = f(\|x - x'\|) \tag{14}$$

By using an ARD kernel, it is possible to use separate length scales on different dimensions. The length scales are utilized to determine the relevance of an input and, consequently, it can be used to remove irrelevant inputs [51]. The sum of the radial basis function (RBF) in (15) and the rational quadratic (RQ) kernel in (16) is used. s_{noise} is the noise variance, $diag(\frac{1}{l})$ a diagonal matrix with the length scales l, α a smoothness factor, and x and x' the data points. While both parts contribute to the ARD effect, the RQ part increases the robustness against outliers.

$$k(x, x') = s_{noise}^2 \cdot e^{-0.5(x-x')^{\top} diag(\frac{1}{l})(x-x')} \tag{15}$$

$$k(x, x') = \left(1 + \frac{\|x - x'\|^2}{2\alpha l^2}\right)^{-\alpha} \tag{16}$$

Different metrics are used to evaluate the performance of the model. The RMSE enhances the impact of larger errors, while the impact of different error values is the same for the MAE. The used metrics with the real target values y_i and the estimated target values y_i^* are shown in the following:

$$RMSE(y_i, y_i^*) = \sqrt{\frac{1}{n}\sum_{i=1}^{n}(y_i - y_i^*)^2} \tag{17}$$

$$MAE(y_i, y_i^*) = \frac{1}{n}\sum_{i=1}^{n}|y_i - y_i^*| \tag{18}$$

The general procedure to develop the prediction model starting with the raw data till the evaluation of the forecasting results is summarized in Fig. 4. To analyze the reliability and robustness of the prediction, the model is retrained ten times with a different allocation in training, validation, and test data.

3. Results

To compare the accuracies of the predictive model and the influence of different data processing methods, two different metrics with RMSE and MAE are used. With a varying amount of input data, the risk of overfitting is minimized and features are extracted for the final model.

3.1. Dimension reduction

Two main approaches to extract features for the model can be separated. By selecting a pre-processing method, the data is analyzed and information can be gained from it. The first approach is a PCA. By using this data based dimension reduction method, the variance of the different components is analyzed before the final dimension is selected. Basis for the reduction is the coverage of a broad range of the initial variance of the data. The results with the variance accumulated over the principal components is plotted against the dimension in Fig. 5.

With the usage of five components, a variance range of over 99.99% can be covered. Thus, the final dimension is selected to be 5. In addition, based on the PCA, a classification for the different battery types is possible. The results are visualized in Fig. 6. The SOH is plotted over the first component of the PCA. For reasons of comprehensibility,

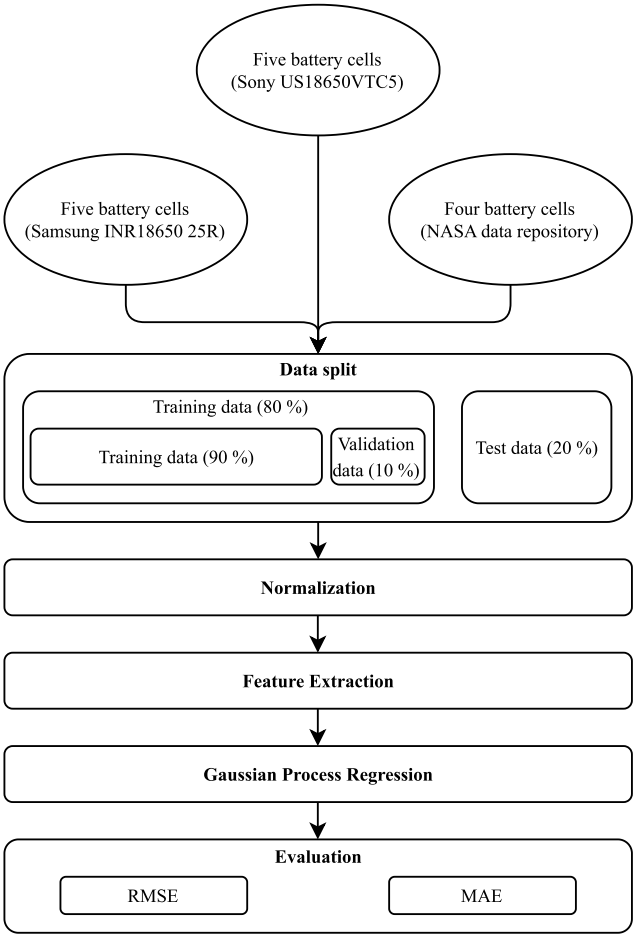

Fig. 4. Flowchart of the methodology and the procedure for developing the prediction model for the SOH of LIBs from data collection over data pre-processing to the forecasting and its evaluation.

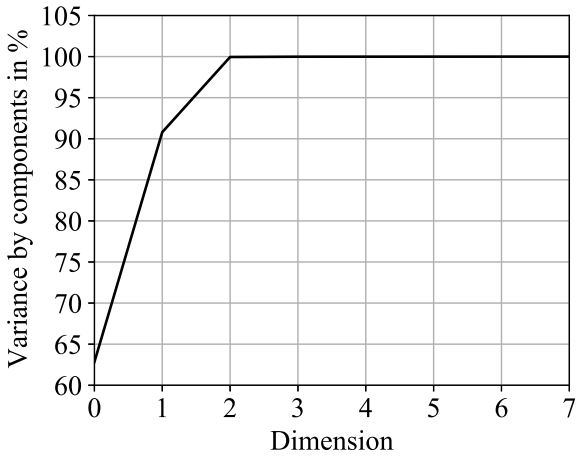

Fig. 5. Accumulated variance of the components using a PCA for different dimensions of the input data. The number of principal components (dimension) is specified on the *x*-axis.

only one principal component is used for the visualization, but as described, five principal components are used for the prediction.

Several aspects are noticeable. Three different areas of data points can be separated. The areas can be allocated to the different battery types. Based on the feature data, it is possible to categorize the data without additional information of battery type or cell chemistry. Both

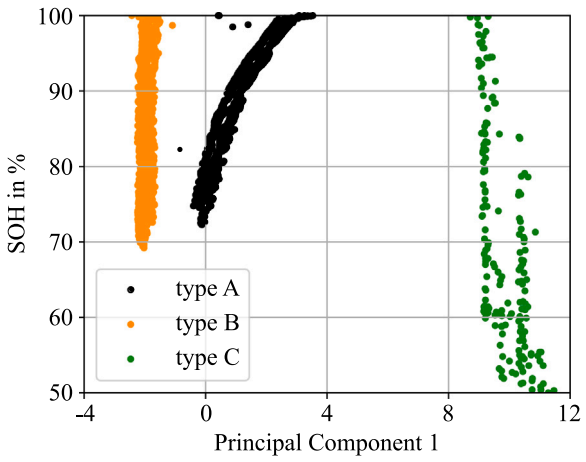

Fig. 6. Comparison of battery data sources using the PCA. The SOH is plotted over the first principal component. The three different sources can be separated based on the variance of the data.

Table 1
Results of the State-of-Health prediction with the oversampling method and re-training the model ten times.

Metric	Mean error	Standard deviation
RMSE train	7.492	0.196
RMSE validation	11.171	1.834
RMSE test	8.993	3.147
MAE train	1.369	0.065
MAE validation	6.857	2.305
MAE test	6.862	2.837

dense prediction areas on the left and in the middle are data points from the own dataset without the random charging and discharging cycles. The third area contains the data points from the public dataset. The data is compared to the other two battery types wider distributed and it covers a higher SOH range.

3.2. Prediction model

The data of 14 battery cells is used to predict the SOH. Considering the different battery types and loading conditions, it results in a high variety of the data and impedes the prediction. To tackle this problem, an oversampling strategy is applied to enrich the dataset. The SMOGN algorithm is used. It is adapted from the SMOTE algorithm, which was originally developed for classification tasks. Instead of increasing the accuracy of the model, it was deteriorated. The main problem of the oversampling method, which is based on a k-Nearest-Neighbor technique, are the battery parameters current, voltage, and temperature. They are internally correlated and affect the SOH of a battery cell in different ways. This complicates the prediction task and the possibility to add artificial data without expert knowledge. Next to the accuracy of the model, the robustness is analyzed by means of the resulting standard deviation by re-training the model ten times. The results are summarized in Table 1.

Regardless of the evaluated battery type, the oversampling strategy leads to higher errors in the SOH prediction. While increasing the error for the battery type A and B with the same loading conditions by approximately 0.3%, the addition of the public dataset with a higher variety of loading conditions impairs the accuracy with the oversampling method by 6.3%. Despite the increase of training data with the oversampling method by 30%, the training speed could be reduced by approximately 10%.

Nevertheless, compared to the results of the model without oversampling, shown in Table 2, the errors are higher. The same results are

Table 2
Results of the State-of-Health prediction with the PCA, ten times re-trained model.

Metric	Mean error	Standard deviation
RMSE train	2.793	0.6448
RMSE validation	3.005	0.146
RMSE test	3.039	0.301
MAE train	1.398	0.327
MAE validation	1.405	0.083
MAE test	1.431	0.152

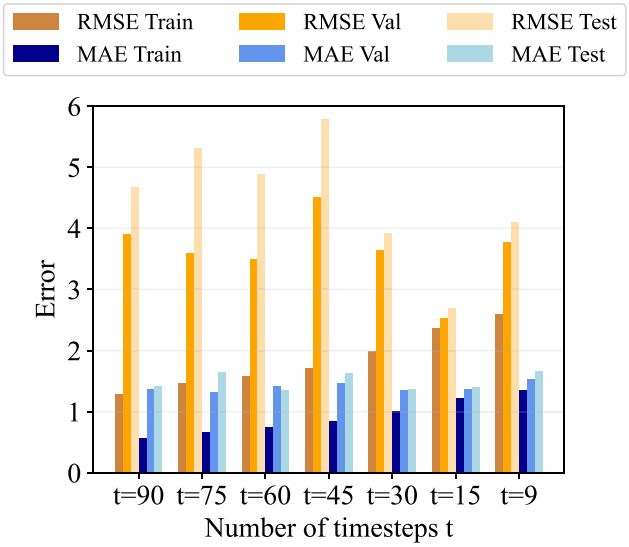

Fig. 7. Comparison of the prediction errors based on RMSE and MAE for varying input features divided in training, validation, and test error. The timesteps t included for the prediction are indicated on the x-axis.

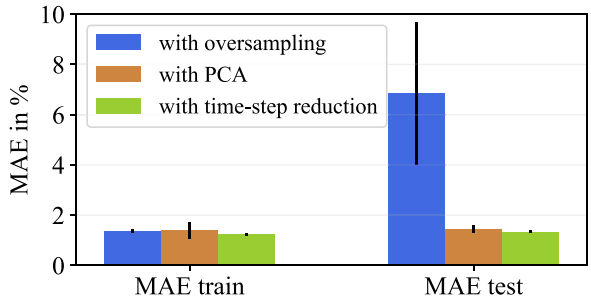

Fig. 8. Comparison of the results of the algorithms with the oversampling strategy, with the PCA, and the final time step reduction method. The MAE for training and test of the model with the corresponding standard deviation for a ten times retrained model is shown.

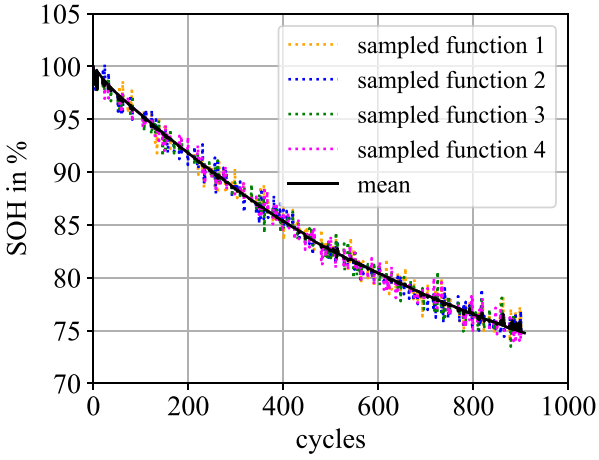

Fig. 9. Exemplary posterior distribution of the GPR for the SOH prediction over cycles with four different samples for one battery cell. The sampled functions and the mean for the SOH are plotted over the discharge cycles.

obtained for the standard deviation, as the model with the oversampling technique shows higher deviations while re-training the model. With the created data points based on the oversampling algorithm, it is not possible to represent the real degradation behavior. Thus, the oversampling method was not used for the final model. Table 2 shows the errors for the model with the PCA. Training and validation errors are close to each other, which indicates that there is no overfitting. The validation data is used to fine-tune the parameters. The test data is unseen for the model. Nevertheless, the error values of the test data are similar to the validation data. This shows the generalizability of the model and the applicability for unseen data.

Next to the PCA, a second dimension reduction method is conducted. The number of included timesteps is decreased to reduce the risk of overfitting. The sensitivity to the number of input features is analyzed. The results for selected number of timesteps is summarized in Fig. 7, where the training, validation, and test errors are plotted over the time sequences included for the prediction.

The results for 15 timesteps show low errors and no indications for overfitting, as the deviations between training and validation error is small. Therefore, 15 timesteps are included to develop the prediction model for the SOH. By further lowering the timesteps, the model error is increasing again and the features are not sufficient to adequately describe the phenomenon. This is typical for underfitting. The comparison between the algorithm with oversampling, with the PCA, and with time step reduction method is summarized based on the MAE of training and test of the model in Fig. 8. All models are retrained ten times and, additionally, the resulting standard deviation is shown as well.

While developing a GPR, a distribution over functions is created. This is called the posterior distribution. The mean values of the functions are used for the actual point prediction. Four exemplary functions of the posterior distribution and the mean for one battery cell are shown in Fig. 9.

Oscillations, both up and down, can be observed for the sampled functions. The fluctuations also vary between the sampled functions, but they are all distributed around the mean curve. On the contrary, the mean function exhibit a smooth decrease over the cycles, which is close to the real data. The mean curve is very similar to a smoothed sample function. It is striking that in the high SOH area the deviations are mainly downwards, while the deviations after that are similar on both sides. The points with no deviations are explainable as they are the grid points used for training the model. To analyze the predictability and the associated uncertainty in detail, the real data, the predicted values, and the 95% confidence interval for the same battery cell are shown in Fig. 10. To calculate the confidence interval, the lower and upper boundaries are calculated with the standard deviation and the factor of |1.96|. Consequently, there is a 5% chance that a data point lies outside the confidence interval. Additionally, an exemplary area is presented in more detail to give a clear visualization of the deviations between real and predicted data with the associated confidence interval.

Within the 95% confidence interval, there are deviations smaller than |2|%. Thus, the uncertainty in the prediction of the model is low and the deviation from the real value is small. The confidence interval is similar over the whole prediction area, which means that the accuracy of the prediction does not change over a decreasing SOH. The predictions and the real data are also overlapping for most of the degradation curve. Higher fluctuations can be observed at a SOH of 75%. This can be explained by the data, where the edge regions are not as represented as the other areas, and by the ageing behavior of a battery cell with an approximately linear decrease at high SOHs and a faster decrease at the areas of a lower SOH. The zoom-in shows an

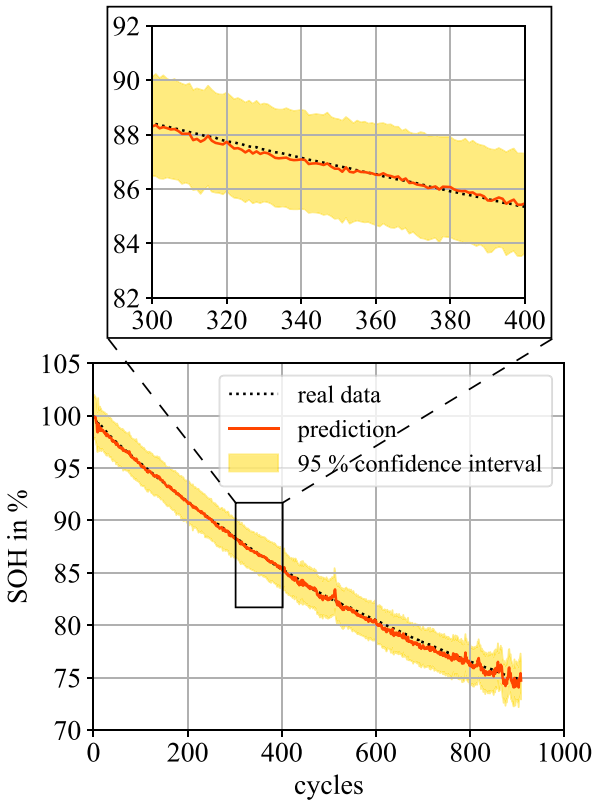

Fig. 10. Results of the GPR for one battery cell with the real data, the prediction, and the 95% confidence interval. The zoom-in shows both the deviations between the real data and the prediction of the model, as well as the range of the 95% confidence interval in more detail.

Table 3
Results of the State-of-Health prediction with the final, ten times re-trained model.

Metric	Mean error	Standard deviation
RMSE train	2.376	0.130
RMSE validation	2.478	0.196
RMSE test	2.777	0.361
MAE train	1.226	0.058
MAE validation	1.305	0.114
MAE test	1.330	0.042

exemplary area between cycle 300 and 400. It can be observed that the prediction and the real data are very similar for most of the data points. Small fluctuations in the forecasting results lead to increased errors and, overall, the prediction curve exhibits more noise. The magnitude of the noise is small, as intended through the kernel function. All in all, the predictability over the whole covered area can be shown. To further evaluate the model, different metrics are calculated. The resulting RMSE and MAE for training, validation, and test of the final model are summarized in Table 3. The model was retrained ten times to analyze the robustness. The mean values and the standard deviation are listed.

The metrics for the validation error were used to optimize the hyperparameter of the model. The testing data set was not used in the development of the model. Indeed, the testing metrics show only slightly worse results than the validation errors. This means that it is possible for the model to predict the SOH for unseen data, resulting in a MAE under 1.5%. The combined kernel function to approximate the long term and the short term behavior of the battery degradation is suitable. As the validation and test errors are similar, the calculated function between input features current, voltage, and temperature and the SOH is generalizable. It is possible to train the model for different types of battery cells, which, in this case, are all cylindrical LIBs of the form 18 650. By combining the data, the developed model can accurately predict the decreasing capacity. Based on the standard deviations for retraining the model ten times, it shows robust behavior. This shows the general applicability of the GPR for degradation forecasting of LIBs. Further, the standard deviation for retraining the models is low. Reason for the deviation of the results is the random split in training, validation, and test data. Consequently, the data basis is sufficient for this scope of SOH prediction. Compared to models in the literature, similar to lower errors can be obtained. While these models are only applicable to a single cell type, the presented model is trained, validated, and tested for different operating conditions for three different battery types. While the mean training error is a MAE of 1.226%, the test MAE is obtained with a value of 1.33%. It demonstrates the high accuracy for unseen data. In addition, the confidence interval shows the high reliability of the prediction using a GPR.

4. Discussion

A major challenge in ensuring a reliable operation of battery cells is the determination of the condition. Conventional battery models require high computational power or exhibit lower accuracies. There is high potential of using data-driven predictive models, especially for probability models with uncertainty values for the results. The usage and optimization of a GPR to forecast the SOH of a LIB from data pre-processing to the final ML model is discussed, as well as the applicability and flexibility for different battery types.

4.1. Data processing

Several aspects have to be considered applying data pre-processing methods. Two main areas can be separated. The first one is the dimension reduction to minimize the risk of overfitting, while retaining important features. The second one is data augmentation, which is the artificial creation of additional data to train the ML model. By using these methods, the complexity and the necessary computing power should be kept low. Thus, the preferable aim of this data-driven model is to use the measured values with current, voltage, and temperature to reduce the pre-processing efforts for the model inputs. Compared to other ML models, the impact of overfitting of a GPR is small, but it can be determined. By using the raw data as input in the model, the model tends to overfit. This can be seen in the higher deviations between training and validation errors for higher numbers of included timesteps. This trend is also increasing using higher dimensions, which is typical for overfitting. Therefore, a dimension reduction method is important to improve the model. The utilization of a PCA is reasonable and leads to lower prediction errors. Drawbacks are the development time while keeping the balance between dimension reduction and excluding important information, as well as the additional calculation step in the final model. In comparison, a reduction of included timesteps results in slightly higher improvements. The model benefits from using time series data of the battery parameters and, hence, the high intercorrelation in the data can be exploited. Therefore, a feature reduction based on the timesteps is possible. The complexity of the model is reduced and the storage requirements for historical data can be kept low, which is also beneficial for an application. A ML model is highly dependent on its data basis. To improve that, data can be artificially created using data augmentation techniques. Because battery aging tests are time- and cost-intensive, data augmentation could be an alternative to improve data driven models. There are several approaches, but nearly all of the methods are developed for image processing and the possibilities for a regression are rare. In this case, the SMOGN algorithm is used to enrich the data basis. This approach is based on the present data and does not include electrochemical knowledge or simulations. Therefore, the method, which is evolved from the k-Nearest Neighbor algorithm, is depending on the arbitrary number of dimension. In addition to that,

the intercorrelation impedes the problem because the data points are very similar. The impact of the parameters on the current condition is evident in varying degrees and different combinations of battery parameters can lead to the same battery condition. The same phenomenon could be observed for the data with constant loading and for the data with higher variety in the loading conditions. Nevertheless, the training speed could be reduced by using the oversampling method. This is an indicator that the enlargement of the dataset could lead to a better approximation of the correlation between the input features and the SOH. It is expected that the SMOGN algorithm can improve the prediction if the data can represent several loading conditions. However, it is a time-consuming process to find the optimal parameters, as each artificially created data point is highly depending on the real data points next to it. In this case, the data augmentation technique is not improving the prediction results, and it is therefore not used in the final model.

4.2. SOH prediction

Three different battery types are combined to create the prediction model for the SOH of LIBs. In addition to that, the cells are aged under different cycling conditions. As this is the case for real applications, aim is to approximate the ageing behavior under different conditions and for different cells. Even if the innovations in the battery sector are mostly incremental and not disruptive, battery models need a new parameterization and are only applicable to one specific battery type. The increasing complexity stands in contrast to the advantage of using the same model for different cell chemistries, which would not only benefit an application, but also enhances the options of training data-driven models, as battery ageing experiments are time and cost intensive and, thus, degradation data of LIBs are rare.

With the GPR, it is possible to combine different battery types for a single forecasting model. All battery types are approximately aged to a SOH between 50 and 70%. Nevertheless, the battery types show different data distributions, though they can be accurately approximated. The random loading conditions and, therefore, the sparse data situation for a single operating condition impedes the SOH prediction. Even though the ML model has no information about the battery types, it can predict the SOH with high accuracies. By changing the cell type and adapting to technological developments, a new parameterization of the battery models is usually necessary. This is a time consuming process and sometimes not possible, as in an early stage, the data foundation is neither reliable nor representative for the various environmental and working conditions of a battery. It is shown that a new parameterization of the model is not necessary by using a GPR. It is possible to separate the different cell types by analyzing the variance in the data. The complex search for hyperparameters for data driven models can be avoided while maintaining high accuracies. Similar to and based on the idea of transfer learning, the ML model is retrained by different cell types. They are combined to improve the overall performance. It could be shown that the prediction for different battery types is possible using a single model. However, the used battery types are similar and the behavior for batteries with higher discrepancies has to be examined. Further, the evaluated operating conditions are limited, which impedes the applicability in a real world scenario. Compared to the initial model, in which a whole discharge cycle is used to estimate the SOH, the final model utilizes only the last 15 time steps during discharge. In an application under complex charging and discharging conditions, it is almost never possible to consider a whole discharge cycle. However, in the final model only the last time steps representing the low SOC area are used for the estimation. This would benefit an application and would further reduce the computing efforts in a BMS. The limited variations of loading conditions impede the scope of application. Nevertheless, the proposed algorithm shows high accuracies for the data in the laboratory environment and is expected to show similar behavior while trained with data with a higher relation to real loading conditions. All in all, compared to other SOH estimation techniques, be they electrochemical, model-based, or data-driven approaches, the accuracy is similar while the development time is lower and the model parameters do not change over the battery lifetime [52,53]. While comparing the proposed algorithm with GPR models from the literature, several points are striking. The first one is the feature extraction. Instead of using the measured data during the battery loading, features are often elaborately extracted from the data [54,55]. After extracting seven features from their initial data set, consisting mainly of the internal resistance and time of constant current phase, Yang et al. compared different data-driven methods based on their accuracy [56]. The mean absolute errors of the support vector machine as well as the deep neural network and the long short-term memory neural network vary between 1 and 3%. With the GPR and the deep GPR, it was possible to reduce the error below 1%. Next to that, features based on the data of the electrochemical impedance spectroscopy (EIS) are utilized resulting in similar accuracies [57]. Further, the influence of a suitable kernel function was quantified. While varying the ARD kernel with the squared exponential and the Matern kernel, the error values differ around 1%. This denotes the importance of the kernel choice. All in all, these methods require higher pre-processing efforts by the BMS while extracting the features in those approaches and are suitable for one battery type. The accuracies of the algorithms vary depending on the loading conditions and final structure of the kernel, but reach similar error values around 1%. The proposed model, however, reduces efforts for data recording and pre-processing the data. Further, it can be used for different battery types, which is important when there is a higher variety of battery types in an electric vehicle that can be used. Next to that, the accuracy of the model is similar to the comparable models in the literature. However, the applicability on highly dynamic loading conditions has to be evaluated in the future.

The dataset consists of 14 battery cells. The prediction ability for the unseen testing data is clearly visible. The accuracy is better in the mean areas, which can be explained in the distribution of the data. The main potential for optimizing the prediction model lies in the edge regions, especially in the high SOH area, which is underrepresented in the dataset. Further, outliers could be detected for the own and the public dataset. While the outliers from the own dataset could be predicted accurately, the outliers of the public dataset are leading to the highest error. Enriching the data distribution in these regions could improve the prediction quality. The usage of an oversampling method based on the kNN algorithm did not lead to an improvement of the forecasting results. However, an advanced oversampling strategy could also lead to beneficial results. The use of expert knowledge and information about the aging behavior in the oversampling strategy could be a solution. In comparison between battery type and loading conditions, the loading conditions can clearly be identified as the critical factor. By applying the PCA, the battery types can be classified and the prediction accuracy could be improved. The variety of the random loading conditions still lead to higher errors. To approximate the aging behavior, an ARD kernel is used. By using different length scales, the dimensions of the problems can be decoupled and, therefore, it is possible to concentrate on the relevant features. In certain areas, the mean function is slightly fluctuating around the real value. Therefore, the zero mean prior is suitable for the model, as in another case, the prediction curve would only be dragged down in comparison to the real values. The uncertainty of the prediction is similar across the whole cycle life, which indicates that appropriate lengthscales are used in the model. The aging behaviors can be captured by the model. The deviations of the mean function in the edge areas influence the uncertainty of the prediction, but the range of the uncertainty interval stays nearly the same. All in all, the forecasting model results in accuracies higher than 98% and it performs well under similar operating conditions. Potentials for improvement are the predictions based on extreme loading conditions.

5. Conclusion

Data driven approaches with statistical or ML algorithms are not only a good alternative to determine the condition of a battery, but they also show high accuracies when they are trained on a large and reliable data set. The intertwined battery parameters, which influence each other and the degradation process, complicate the application of oversampling strategies and are only partly applicable for optimizing a forecasting model for the SOH. In contrast, it is possible to combine the prediction for different battery cells under different operating conditions in a single model. Even though the model is usable for three different cell types, which increases the complexity, the lowest test error was obtained with an MAE of 1.33%. The main driver for higher errors could be identified as the random loading conditions during the ageing of the batteries. Despite the sparse data distribution for a single loading condition, it is possible to predict the SOH with low errors. The adaptability for different battery types is a key advantage for an application. Compared to the validation errors, the developed model shows good results on unseen testing data. The uncertainties of the forecasting method are low and it shows robust behavior. In the future, it is planned to test the model against a higher variety of loading conditions and to optimize the model in regards to different cell chemistries and the predictability in the edge regions of the SOH, as well as extreme operating conditions. Further optimization potential lies in the data pre-processing step for an efficient extraction of features. Aim is to reduce the needed computing power while increasing the prediction accuracy and improving the approximation of the ageing behavior of LIBs under different conditions.

CRediT authorship contribution statement

Sebastian Pohlmann: Writing – review & editing, Writing – original draft, Visualization, Validation, Software, Resources, Methodology, Investigation, Formal analysis, Data curation, Conceptualization. **Ali Mashayekh:** Writing – review & editing, Validation, Methodology, Investigation, Formal analysis, Conceptualization. **Florian Stroebl:** Writing – review & editing, Resources, Methodology, Investigation, Data curation. **Dominic Karnehm:** Validation, Software, Investigation, Formal analysis. **Manuel Kuder:** Writing – review & editing, Supervision, Project administration, Funding acquisition. **Antje Neve:** Writing – review & editing, Visualization, Supervision, Project administration, Funding acquisition, Formal analysis. **Thomas Weyh:** Writing – review & editing, Supervision, Project administration, Funding acquisition.

Declaration of competing interest

The authors declare that they have no known competing financial interests or personal relationships that could have appeared to influence the work reported in this paper.

Data availability

Data will be made available on request.

Acknowledgments

This research [project MORE] is funded by dtec.bw – Digitalization and Technology Research Center of the Bundeswehr, Germany, which we gratefully acknowledge. dtec.bw is funded by the European Union – NextGenerationEU. Further, we thank Markus Spielbauer for obtaining the experimental data.

References

[1] Johannes Buberger, Anton Kersten, Manuel Kuder, Richard Eckerle, Thomas Weyh, Torbjörn Thiringer, Total CO2-equivalent life-cycle emissions from commercially available passenger cars, Renew. Sustain. Energy Rev. 159 (2022) 112158, http://dx.doi.org/10.1016/j.rser.2022.112158, URL https://www.sciencedirect.com/science/article/pii/S1364032122000867.

[2] Sandro Stock, Sebastian Pohlmann, Florian J. Günter, Lucas Hille, Jan Hagemeister, Gunther Reinhart, Early quality classification and prediction of battery cycle life in production using machine learning, J. Energy Storage 50 (2022) 104144, http://dx.doi.org/10.1016/j.est.2022.104144, URL https://www.sciencedirect.com/science/article/pii/S2352152X22001785.

[3] Ghassan Zubi, Rodolfo Dufo-López, Monica Carvalho, Guzay Pasaoglu, The lithium-ion battery: State of the art and future perspectives, Renew. Sustain. Energy Rev. 89 (2018) 292–308, http://dx.doi.org/10.1016/j.rser.2018.03.002, URL https://www.sciencedirect.com/science/article/pii/S1364032118300728.

[4] Wladislaw Waag, Christian Fleischer, Dirk Uwe Sauer, Critical review of the methods for monitoring of lithium-ion batteries in electric and hybrid vehicles, J. Power Sources 258 (2014) 321–339, http://dx.doi.org/10.1016/j.jpowsour.2014.02.064, URL https://www.sciencedirect.com/science/article/pii/S0378775314002572.

[5] Shulin Liu, Xia Dong, Xiaodong Yu, Xiaoqing Ren, Jinfeng Zhang, Rui Zhu, A method for state of charge and state of health estimation of lithium-ion battery based on adaptive unscented Kalman filter, Energy Rep. 8 (2022) 426–436, http://dx.doi.org/10.1016/j.egyr.2022.09.093, URL https://www.sciencedirect.com/science/article/pii/S2352484722018170.

[6] Akash Basia, Zineb Simeu-Abazi, Eric Gascard, Peggy Zwolinski, Review on State of Health estimation methodologies for lithium-ion batteries in the context of circular economy, CIRP J. Manuf. Sci. Technol. 32 (2021) 517–528, http://dx.doi.org/10.1016/j.cirpj.2021.02.004, URL https://www.sciencedirect.com/science/article/pii/S1755581721000249.

[7] J. Estaller, A. Kersten, M. Kuder, A. Mashayekh, J. Buberger, T. Thiringer, R. Eckerle, T. Weyh, Battery impedance modeling and comprehensive comparisons of state-of-the-art cylindrical 18650 battery cells considering cells' price, impedance, specific energy and C-rate, in: 2021 IEEE International Conference on Environment and Electrical Engineering and 2021 IEEE Industrial and Commercial Power Systems Europe, EEEIC / I&CPS Europe, 2021, pp. 1–8, http://dx.doi.org/10.1109/EEEIC/ICPSEurope51590.2021.9584562.

[8] Zhong Ren, Changqing Du, A review of machine learning state-of-charge and state-of-health estimation algorithms for lithium-ion batteries, Energy Rep. 9 (2023) 2993–3021, http://dx.doi.org/10.1016/j.egyr.2023.01.108, URL https://www.sciencedirect.com/science/article/pii/S235248472300118X.

[9] Manh-Kien Tran, Manoj Mathew, Stefan Janhunen, Satyam Panchal, Kaamran Raahemifar, Roydon Fraser, Michael Fowler, A comprehensive equivalent circuit model for lithium-ion batteries, incorporating the effects of state of health, state of charge, and temperature on model parameters, J. Energy Storage 43 (2021) 103252, http://dx.doi.org/10.1016/j.est.2021.103252, URL https://www.sciencedirect.com/science/article/pii/S2352152X2100949X.

[10] Jianfeng Wang, Yongkai Jia, Na Yang, Yanbing Lu, Mengyu Shi, Xutong Ren, Dongchen Lu, Precise equivalent circuit model for Li-ion battery by experimental improvement and parameter optimization, J. Energy Storage 52 (2022) 104980, http://dx.doi.org/10.1016/j.est.2022.104980, URL https://www.sciencedirect.com/science/article/pii/S2352152X22009859.

[11] Huixin Tian, Pengliang Qin, Kun Li, Zhen Zhao, A review of the state of health for lithium-ion batteries: Research status and suggestions, J. Clean. Prod. 261 (2020) 120813, http://dx.doi.org/10.1016/j.jclepro.2020.120813, URL https://www.sciencedirect.com/science/article/pii/S095965262030860X.

[12] Rui Xiong, Linlin Li, Jinpeng Tian, Towards a smarter battery management system: A critical review on battery state of health monitoring methods, J. Power Sources 405 (2018) 18–29, http://dx.doi.org/10.1016/j.jpowsour.2018.10.019, URL https://www.sciencedirect.com/science/article/pii/S037877531831111X.

[13] K. Severson, P. Attia, N. Jin, N. Perkins, B. Jiang, Z. Yang, M. Chen, M. Aykol, P. Herring, D. Fraggedakis, M. Bazant, S. Harris, W. Chueh, R. Braatz, Data-driven prediction of battery cycle life before capacity degradation, Nat. Energy 4 (2019) 1–9, http://dx.doi.org/10.1038/s41560-019-0356-8.

[14] J. Zhu, Y. Wang, Y. Huang, R. Bhushan Gopaluni, Y. Cao, M. Heere, M.J. Mühlbauer, L. Mereacre, H. Dai, X. Liu, A. Senyshyn, X. Wei, M. Knapp, H. Ehrenberg, Data-driven capacity estimation of commercial lithium-ion batteries from voltage relaxation, Nature Commun. 13 (1) (2022) 2261, http://dx.doi.org/10.1038/s41467-022-29837-w.

[15] Minzhi Chen, Guijun Ma, Weibo Liu, Nianyin Zeng, Xin Luo, An overview of data-driven battery health estimation technology for battery management system, Neurocomputing 532 (2023) 152–169, http://dx.doi.org/10.1016/j.neucom.2023.02.031, URL https://www.sciencedirect.com/science/article/pii/S0925231223001686.

[16] H. Dai, G. Zhao, M. Lin, J. Wu, G. Zheng, A novel estimation method for the state of health of lithium-ion battery using prior knowledge-based neural network and Markov chain, IEEE Trans. Ind. Electron. 66 (10) (2019) 7706–7716, http://dx.doi.org/10.1109/TIE.2018.2880703.

[17] S. Sahoo, K.S. Hariharan, S. Agarwal, S.B. Swernath, R. Bharti, S. Han, S. Lee, Transfer learning based generalized framework for state of health estimation of Li-ion cells, Sci. Rep. 12 (1) (2022) 13173, http://dx.doi.org/10.1038/s41598-022-16692-4.

[18] Shuzhi Zhang, Baoyu Zhai, Xu Guo, Kaike Wang, Nian Peng, Xiongwen Zhang, Synchronous estimation of state of health and remaining useful lifetime for lithium-ion battery using the incremental capacity and artificial neural networks, J. Energy Storage 26 (2019) 100951, http://dx.doi.org/10.1016/j.est.2019.100951, URL https://www.sciencedirect.com/science/article/pii/S2352152X19307340.

[19] Jiachi Yao, Te Han, Data-driven lithium-ion batteries capacity estimation based on deep transfer learning using partial segment of charging/discharging data, Energy 271 (2023) 127033, http://dx.doi.org/10.1016/j.energy.2023.127033, URL https://www.sciencedirect.com/science/article/pii/S0360544223004279.

[20] Penghua Li, Zijian Zhang, Qingyu Xiong, Baocang Ding, Jie Hou, Dechao Luo, Yujun Rong, Shuaiyong Li, State-of-health estimation and remaining useful life prediction for the lithium-ion battery based on a variant long short term memory neural network, J. Power Sources 459 (2020) 228069, http://dx.doi.org/10.1016/j.jpowsour.2020.228069, URL https://www.sciencedirect.com/science/article/pii/S0378775320303724.

[21] Guijun Ma, Yong Zhang, Cheng Cheng, Beitong Zhou, Pengchao Hu, Ye Yuan, Remaining useful life prediction of lithium-ion batteries based on false nearest neighbors and a hybrid neural network, Appl. Energy 253 (2019) 113626, http://dx.doi.org/10.1016/j.apenergy.2019.113626, URL https://www.sciencedirect.com/science/article/pii/S0306261919313005.

[22] Xiaoyu Li, Changgui Yuan, Xiaohui Li, Zhenpo Wang, State of health estimation for Li-Ion battery using incremental capacity analysis and Gaussian process regression, Energy 190 (2020) 116467, http://dx.doi.org/10.1016/j.energy.2019.116467, URL https://www.sciencedirect.com/science/article/pii/S0360544219321620.

[23] M.S. Hossain Lipu, M.A. Hannan, Aini Hussain, M.M. Hoque, Pin J. Ker, M.H.M. Saad, Afida Ayob, A review of state of health and remaining useful life estimation methods for lithium-ion battery in electric vehicles: Challenges and recommendations, J. Clean. Prod. 205 (2018) 115–133, http://dx.doi.org/10.1016/j.jclepro.2018.09.065, URL https://www.sciencedirect.com/science/article/pii/S0959652618327793.

[24] Xiaoyu Li, Zhenpo Wang, Jinying Yan, Prognostic health condition for lithium battery using the partial incremental capacity and Gaussian process regression, J. Power Sources 421 (2019) 56–67, http://dx.doi.org/10.1016/j.jpowsour.2019.03.008, URL https://www.sciencedirect.com/science/article/pii/S0378775319302393.

[25] Jianbo Yu, State of health prediction of lithium-ion batteries: Multiscale logic regression and Gaussian process regression ensemble, Reliab. Eng. Syst. Saf. 174 (2018) 82–95, http://dx.doi.org/10.1016/j.ress.2018.02.022, URL https://www.sciencedirect.com/science/article/pii/S095183201730652X.

[26] Fan Li, Jiuping Xu, A new prognostics method for state of health estimation of lithium-ion batteries based on a mixture of Gaussian process models and particle filter, Microelectron. Reliab. 55 (7) (2015) 1035–1045, http://dx.doi.org/10.1016/j.microrel.2015.02.025, URL https://www.sciencedirect.com/science/article/pii/S0026271415000906.

[27] Wendi Guo, Zhongchao Sun, Søren Byg Vilsen, Jinhao Meng, Daniel Ioan Stroe, Review of "grey box" lifetime modeling for lithium-ion battery: Combining physics and data-driven methods, J. Energy Storage 56 (2022) 105992, http://dx.doi.org/10.1016/j.est.2022.105992, URL https://www.sciencedirect.com/science/article/pii/S2352152X22019806.

[28] R.R. Richardson, M.A. Osborne, D.A. Howey, Battery health prediction under generalized conditions using a Gaussian process transition model, J. Energy Storage 23 (2019) 320–328, http://dx.doi.org/10.1016/j.est.2019.03.022, URL https://www.sciencedirect.com/science/article/pii/S2352152X18307734.

[29] H. Feng, G. Shi, SOH and RUL prediction of Li-ion batteries based on improved Gaussian process regression, J. Power Electron. 21 (12) (2021) 1845–1854, http://dx.doi.org/10.1007/s43236-021-00318-5.

[30] Duo Yang, Xu Zhang, Rui Pan, Yujie Wang, Zonghai Chen, A novel Gaussian process regression model for state-of-health estimation of lithium-ion battery using charging curve, J. Power Sources 384 (2018) 387–395, http://dx.doi.org/10.1016/j.jpowsour.2018.03.015, URL https://www.sciencedirect.com/science/article/pii/S0378775318302398.

[31] Piyush Tagade, Krishnan S. Hariharan, Sanoop Ramachandran, Ashish Khandelwal, Arunava Naha, Subramanya Mayya Kolake, Seong Ho Han, Deep Gaussian process regression for lithium-ion battery health prognosis and degradation mode diagnosis, J. Power Sources 445 (2020) 227281, http://dx.doi.org/10.1016/j.jpowsour.2019.227281, URL https://www.sciencedirect.com/science/article/pii/S0378775319312741.

[32] S. Greenbank, D. Howey, Automated feature extraction and selection for data-driven models of rapid battery capacity fade and end of life, IEEE Trans. Ind. Inform. 18 (5) (2022) 2965–2973, http://dx.doi.org/10.1109/TII.2021.3106593.

[33] K. Liu, Y. Li, X. Hu, M. Lucu, W.D. Widanage, Gaussian process regression with automatic relevance determination kernel for calendar aging prediction of lithium-ion batteries, IEEE Trans. Ind. Inform. 16 (6) (2020) 3767–3777, http://dx.doi.org/10.1109/TII.2019.2941747.

[34] M. Lucu, E. Martinez-Laserna, I. Gandiaga, K. Liu, H. Camblong, W. Widanage, J. Marco, Data-driven nonparametric Li-ion battery ageing model aiming at learning from real operation data - Part B: Cycling operation, J. Energy Storage 30 (2020) 101410, http://dx.doi.org/10.1016/j.est.2020.101410, URL https://www.sciencedirect.com/science/article/pii/S2352152X19314239.

[35] F. Garay, W. Huaman, J. Munoz, Verification and validation of the Gaussian process regression model to predict the state of health in lithium-ion batteries, in: 2022 IEEE XXIX International Conference on Electronics, Electrical Engineering and Computing, INTERCON, 2022, pp. 1–4, http://dx.doi.org/10.1109/INTERCON55795.2022.9870158.

[36] Y. Che, X. Hu, X. Lin, J. Guo, R. Teodorescu, Health prognostics for lithium-ion batteries: mechanisms, methods, and prospects, Energy Environ. Sci. 16 (2) (2023) 338–371, http://dx.doi.org/10.1039/D2EE03019E.

[37] Rui Xiong, Yue Pan, Weixiang Shen, Hailong Li, Fengchun Sun, Lithium-ion battery aging mechanisms and diagnosis method for automotive applications: Recent advances and perspectives, Renew. Sustain. Energy Rev. 131 (2020) 110048, http://dx.doi.org/10.1016/j.rser.2020.110048, URL https://www.sciencedirect.com/science/article/pii/S1364032120303397.

[38] M. Spielbauer, J. Soellner, P. Berg, K. Koch, P. Keil, C. Rosenmüller, O. Bohlen, A. Jossen, Experimental investigation of the impact of mechanical deformation on aging, safety and electrical behavior of 18650 lithium-ion battery cells, J. Energy Storage 55 (2022) 105564, http://dx.doi.org/10.1016/j.est.2022.105564.

[39] B. Bole, C. Kulkarni, M. Daigle, Randomized battery usage data set, https://www.nasa.gov/content/prognostics-center-of-excellence-data-set-repository.

[40] B. Bole, C. Kulkarni, M. Daigle, Adaptation of an electrochemistry-based li-ion battery model to account for deterioration observed under randomized use, 2014.

[41] F. Zhang, T.L. Lai, B. Rajaratnam, N.R. Zhang, Stanford University. Department of Statistics, Cross-validation and Regression Analysis in High-dimensional Sparse Linear Models, Stanford University, 2011.

[42] H. Yanai, K. Takeuchi, Y. Takane, Projection Matrices, Generalized Inverse Matrices, and Singular Value Decomposition, first ed., in: Statistics for Social and Behavioral Sciences, Springer New York, New York, NY, 2011.

[43] N. Kunz, SMOGN: Synthetic minority over-sampling technique for regression with Gaussian noise, 2020, URL https://pypi.org/project/smogn/.

[44] L. Torgo, R. Ribeiro, Utility-based regression, in: J.N. Kok, J. Koronacki, R. Lopez de Mantaras, S. Matwin, D. Mladenič, A. Skowron (Eds.), Knowledge Discovery in Databases: PKDD 2007, Springer Berlin Heidelberg, Berlin, Heidelberg, 2007, pp. 597–604.

[45] L. Torgo, R. Ribeiro, B. Pfahringer, P. Branco, SMOTE for Regression, vol. 8154, 2013, pp. 378–389, http://dx.doi.org/10.1007/978-3-642-40669-0_33.

[46] P. Branco, L. Torgo, R.P. Ribeiro, SMOGN: a pre-processing approach for imbalanced regression, in: P.B. Luís Torgo, N. Moniz (Eds.), Proceedings of the First International Workshop on Learning with Imbalanced Domains: Theory and Applications, in: Proceedings of Machine Learning Research, vol. 74, PMLR, 2017, pp. 36–50, URL https://proceedings.mlr.press/v74/branco17a.html.

[47] A. Mallasto, A. Feragen, Wrapped Gaussian process regression on Riemannian manifolds, in: 2018 IEEE/CVF Conference on Computer Vision and Pattern Recognition, CVPR, IEEE Computer Society, Los Alamitos, CA, USA, 2018, pp. 5580–5588, http://dx.doi.org/10.1109/CVPR.2018.00585, URL https://doi.ieeecomputersociety.org/10.1109/CVPR.2018.00585.

[48] D. Dong, A.B. Chan, Generalized Gaussian process models, in: 2013 IEEE Conference on Computer Vision and Pattern Recognition, IEEE Computer Society, Los Alamitos, CA, USA, 2011, pp. 2681–2688, http://dx.doi.org/10.1109/CVPR.2011.5995688, URL https://doi.ieeecomputersociety.org/10.1109/CVPR.2011.5995688.

[49] C. Sammut, G.I. Webb (Eds.), Encyclopedia of Machine Learning and Data Mining, Springer US, Boston, MA, 2017.

[50] M.G. Genton, Classes of kernels for machine learning: A statistics perspective, J. Mach. Learn. Res. 2 (2002) 299–312.

[51] C.E. Rasmussen, Gaussian Processes for Machine Learning, in: Adaptive Computation and Machine Learning, MIT Press, Cambridge, Mass, 2006, URL http://gbv.eblib.com/patron/FullRecord.aspx?p=3338604.

[52] Y. Liu, C. Liu, Y. Liu, F. Sun, J. Qiao, T. Xu, Review on degradation mechanism and health state estimation methods of lithium-ion batteries, J. Traffic Transp. Eng. (Engl. Ed.) 10 (4) (2023) 578–610, http://dx.doi.org/10.1016/j.jtte.2023.06.001, URL https://www.sciencedirect.com/science/article/pii/S2095756423000818.

[53] K. Das, R. Kumar, Electric vehicle battery capacity degradation and health estimation using machine-learning techniques: a review, Clean Energy 7 (6) (2023) 1268–1281, http://dx.doi.org/10.1093/ce/zkad054, arXiv:https://academic.oup.com/ce/article-pdf/7/6/1268/53588600/zkad054.pdf.

[54] Jin Zhao, Li Xuebin, Yu Daiwei, Zhang Jun, Zhang Wenjin, Lithium-ion battery state of health estimation using meta-heuristic optimization and Gaussian process regression, J. Energy Storage 58 (2023) 106319, http://dx.doi.org/10.1016/j.est.2022.106319, URL https://www.sciencedirect.com/science/article/pii/S2352152X22023088.

[55] Sean Buchanan, Curran Crawford, Probabilistic lithium-ion battery state-of-health prediction using convolutional neural networks and Gaussian process regression, J. Energy Storage 76 (2024) 109799, http://dx.doi.org/10.1016/j.est.2023.109799, URL https://www.sciencedirect.com/science/article/pii/S2352152X23031973.

[56] Yalong Yang, Siyuan Chen, Tao Chen, Liansheng Huang, State of health assessment of lithium-ion batteries based on deep Gaussian process regression considering heterogeneous features, J. Energy Storage 61 (2023) 106797, http://dx.doi.org/10.1016/j.est.2023.106797, URL https://www.sciencedirect.com/science/article/pii/S2352152X23001949.

[57] Jia Wang, Rui Zhao, Qiu-An Huang, Juan Wang, Yonghong Fu, Weiheng Li, Yuxuan Bai, Yufeng Zhao, Xifei Li, Jiujun Zhang, High-efficient prediction of state of health for lithium-ion battery based on AC impedance feature tuned with Gaussian process regression, J. Power Sources 561 (2023) 232737, http://dx.doi.org/10.1016/j.jpowsour.2023.232737, URL https://www.sciencedirect.com/science/article/pii/S037877532300112X.